



Deposited via The University of Sheffield.

White Rose Research Online URL for this paper:

<https://eprints.whiterose.ac.uk/id/eprint/188640/>

Version: Accepted Version

---

**Proceedings Paper:**

Yang, Z., Forrester, J., Davidson, J.N. et al. (2022) Resonant current estimation and voltage regulation for piezoelectric transformer-based power supply. In: 11th International Conference on Power Electronics, Machines and Drives (PEMD 2022). PEMD 2022 - The 11th International Conference on Power Electronics, Machines and Drives, 21-23 Jun 2022, Newcastle, UK (hybrid conference). IET Digital Library, pp. 357-361. ISBN: 9781839537189.

<https://doi.org/10.1049/icp.2022.1075>

---

© 2022 IET. This is an author-produced version of a paper accepted for publication in PEMD 2022. Uploaded in accordance with the publisher's self-archiving policy.

**Reuse**

Items deposited in White Rose Research Online are protected by copyright, with all rights reserved unless indicated otherwise. They may be downloaded and/or printed for private study, or other acts as permitted by national copyright laws. The publisher or other rights holders may allow further reproduction and re-use of the full text version. This is indicated by the licence information on the White Rose Research Online record for the item.

**Takedown**

If you consider content in White Rose Research Online to be in breach of UK law, please notify us by emailing [eprints@whiterose.ac.uk](mailto:eprints@whiterose.ac.uk) including the URL of the record and the reason for the withdrawal request.

# Resonant current estimation and voltage regulation for piezoelectric transformer-based power supply

Zijiang Yang<sup>1\*</sup>, Jack Forrester<sup>1</sup>, Jonathan N. Davidson<sup>1</sup>, Martin P. Foster<sup>1</sup>

<sup>1</sup>Department of Electronic and Electrical Engineering, The University of Sheffield, Sir Frederick Mappin Building, Mappin Street, Sheffield, S1 3JD, UK

\* E-mail: zyang53@sheffield.ac.uk

**Keywords:** zero-voltage switching, current estimation, phase-locked loop, piezoelectric transformer, voltage regulation

## Abstract

This paper proposes an output voltage regulation approach for a piezoelectric transformer (PT)-based power converter. The inductorless half-bridge configuration is employed to achieve zero-voltage switching. A resonant current estimation circuit is implemented at the output section of the PT, and it is used by a phase-locked loop (PLL) zero voltage switching (ZVS) controller to synchronise MOSFET switching to the zero crossings of the resonant current. Burst-mode control is employed to provide output voltage regulation of the DC/DC converter. Both experimental and simulation results demonstrate the operation of the system.

## 1. Introduction

Piezoelectric transformer (PT) based resonant converters have been utilised for many applications [1][2][3], and they are considered as a desirable replacement for traditional magnetic transformers. PTs provides high efficiency, high power density, minimal electromagnetic interference and reduced size. PTs are generally constructed from hard piezoelectric materials such as lead-zirconate titanate (PZT), therefore they exhibit high quality factor and low loss.

PT transfers energy between input and output sections using mechanical vibrations. Its input and output capacitance are relatively large because of geometry of the device and thus difficult to achieve zero voltage switching due to insufficient deadtime or charge provided by resonant current, especially without using a series inductor. A critical criteria was developed in [4], which shows that ZVS is guaranteed if the input to output capacitance ratio is below a certain level with  $\pi/2$  deadtime, and the circuit operates at resonance at matched load condition.

Since the resonant current is internal to a PT and cannot be measured directly, the resonant current should be estimated in order to generate a feedback signal. Traditional current estimation methods reported in the literature show good effective sign detection for the resonant current, these methods use either anti-parallel diodes or a voltage differentiator [5][6]. However, they exhibit one or more of the drawbacks: 1) primary estimator implementation could increase total effective capacitance presented at PT input section, making ZVS even more difficult to achieve, 2) the estimated current is sensitive to system noise and could be affected by MOSFET switching events.

Burst-mode modulation has been shown to provide superior performance when compared with pulse-frequency modulation (PFM) and pulse width modulation (PWM) since it provides a higher efficiency and lower harmonics [7][8]. However, traditional burst mode modulation uses a fixed

switching frequency, and this is not desirable for PT-based converter since: 1) load variation is limited due to the narrow control bandwidth, 2) the resonant frequency of the PT will shift due to variations in temperature and load. Therefore, additional compensation is necessary to maximise overall efficiency.

In this work, we propose a phase-locked loop (PLL) controller and burst mode controller with a secondary-side resonant current estimator, to regulate the output voltage while maintaining ZVS operation. By estimating the resonant using only secondary side measurements interference from the MOSFET switching events are avoided improving robustness to noise. The PLL locks onto the estimated resonant current providing a synchronised square wave from which the MOSFET gate signals are derived. Adherence to the critical criterion described in [4] ensures that a particular design can achieve ZVS. The output voltage is regulated through a burst mode controller by adjusting the on/off periods of the switches. The proposed control system is implemented and experimentally validated using a ring dot radial mode PT.

## 2. Description of piezoelectric transformer-based inductorless resonant converter

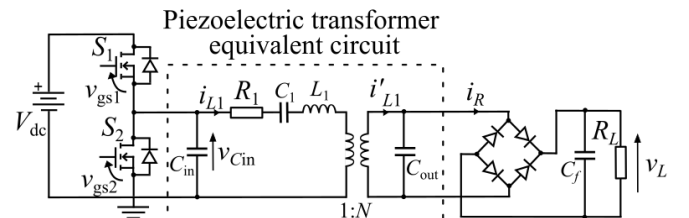


Fig. 1: The inductorless half-bridge driven PT-based converter

Piezoelectric transformers are typically constructed from PZT material and couple energy electromechanically from the input to the output electrodes via mechanical vibrations. High electrical efficiency can be achieved when a PT operates close to its primary resonant frequency due to its high Q factor

nature. The electrical behaviour of a PT can be characterised by the Mason equivalent circuit, as shown in Fig. 1.

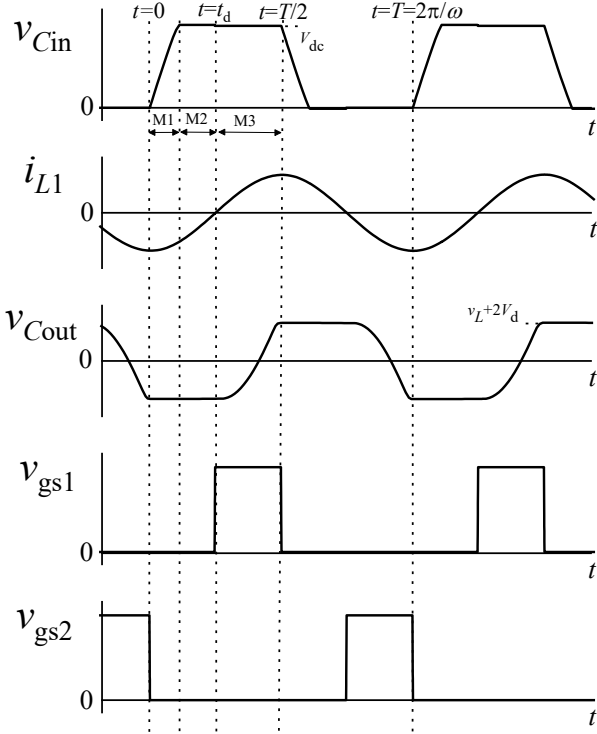


Fig. 2: Switching waveforms of the PT-based converter

During a half-cycle period, the inductorless PT-based converter exhibits three modes of operation (M1, M2 and M3), as shown in Fig. 2. The resonant current is assumed to be sinusoidal since the PT is generally constructed from high Q-factor material.  $t_d$  corresponds to the deadtime. The gate drive signals are represented as  $v_{gs1}$  and  $v_{gs2}$ .  $i_{L1}$  is the current flow at the PT output section and is related to the resonant current  $i_{L1}$  through the ideal transformer which has a ratio 1:N. As can be seen from Fig. 2, ZVS operation is obtained with the following mode sequence M1-M2-M3.

- M1: Both  $S_1$  and  $S_2$  are off. The PT input capacitance-voltage  $v_{cin}$  is charged by resonant current.  $v_{cin}$  is being charged towards  $V_{dc}$  (or heading towards 0V for the negative half-cycle).
- M2:  $v_{cin}$  has exceeded DC link voltage (or fallen below 0V) and the body diode of  $S_1$  (or  $S_2$ ) conducts such that  $v_{cin} = V_f + V_{dc}$  (or  $v_{cin} = -V_f$ ), where  $V_f$  is the forward voltage drop of the body diode.
- M3:  $S_1$  (or  $S_2$ ) is on and  $v_{cin}$  is maintained at  $V_{dc}$  (or 0V). To provide a DC output voltage, a capacitively smoothed full-bridge rectifier is used in this work, since it reduces both geometric constraints of the PT design and conversion ratio requirement for a given output power [9].

To achieve ZVS for an inductorless PT-based converter, both deadtime  $t_d$  and resonant current  $i_{L1}$  should be sufficient to guarantee  $v_{cin}$  charged from 0 to  $V_{dc}$ . In [4], we developed a design criterion to ensure ZVS can always be achieved if the input-to-output capacitance ratio satisfies  $C_{in}/(N^2 C_{out}) \leq 2/\pi$  with  $\pi/2$  deadtime angle, thereby guaranteeing the

deadtime begins at the negative peak of  $i_{L1}$  thereby providing the maximum current to change  $v_{cin}$ .

### 3. Operation of the proposed control system

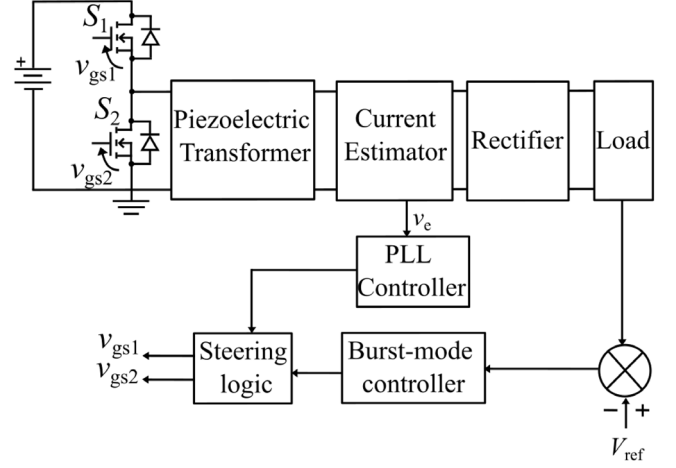


Fig. 3: Circuit block diagram of the proposed control system

The proposed control system includes a resonant estimator, a burst-mode controller and a PLL controller, as shown in Fig. 3. Since the resonant current is internal to the PT and cannot be measured directly, a resonant current estimator is employed after the PT output section, to reconstruct  $i_{L1}$  for the PLL controller. Therefore, the resonant current is locked on by the PLL controller and in-phase gate drive signals are generated through steering logic. Subsequently, the output voltage is rectified and regulated through burst-mode modulation. Finally, the on/off periods of the MOSFETs are dynamically adjusted from the burst-mode signal generated by a hysteresis window with voltage regulation limit.

#### 3.1. Resonant current estimation

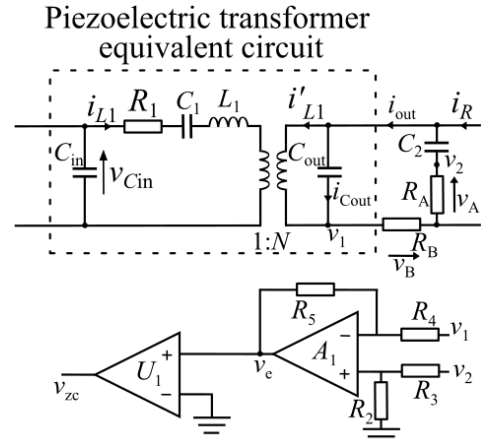


Fig. 4: Resonant current estimation circuit

Since  $i_{L1}$  is a scaled version of the resonant current  $i_{L1}$ , they exhibit the same polarity and, therefore,  $i_{L1}$  can be estimated by combining measurements of output capacitor current  $i_{Cout}$  and PT output current  $i_{out}$ . The two current signals are combined using a differential amplifier  $A_1$ , to provide the current estimate signal  $v_e$ . Comparator  $U_1$  detects the zero-crossing of current estimate which is then provided to the PLL as voltage  $v_{zc}$  for simultaneous phase and frequency

locking. As can be seen from Fig. 4,  $R_A$  senses the PT output capacitor current while  $R_B$  senses the PT output current. Therefore, a scaled version of  $i_{C_{out}}$  and  $i_{out}$  can be generated (if  $R_A C_2 \ll T$  and  $R_B C_{in} \ll T$ , where  $T$  is the switching period) to reconstruct the resonant current  $i_{L1}$ .

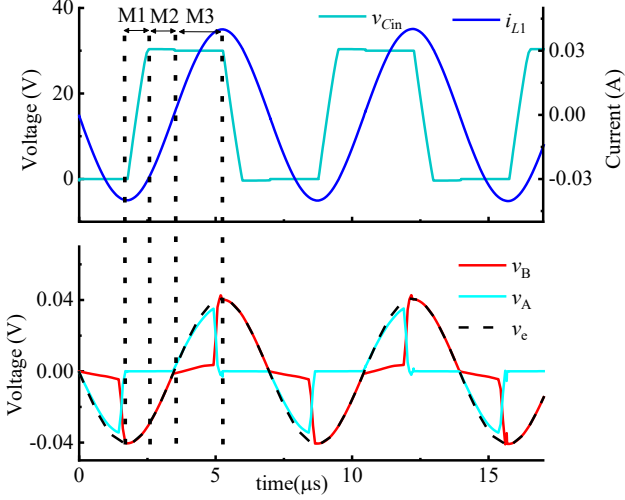


Fig. 5: Switching waveforms of the current estimator

$$i_{L1} = \frac{1}{N} \left( \frac{v_2 C_{out}}{C_2 R_A} - \frac{v_1}{R_B} \right) \quad (1)$$

Therefore, resonant current is estimated as

$$v_e = v_2 \frac{R_2 / (R_3 + R_2)}{R_4 / (R_4 + R_5)} - v_1 \frac{R_5}{R_4} \quad (2)$$

From equation (1) and (2), it is indicated that with careful component selection,  $v_e \propto i_{L1}$

Fig. 5 shows the SPICE simulation waveforms of current estimator under ZVS. During M1 and M2, the bridge rectifier is conducting and so the PT output is clamped to the load voltage  $v_L$  and, therefore,  $i_{C_{out}}$  and its derivative signal  $v_A$  are zero, while PT output current  $i_{out}$  and its scaled version  $v_B$  is dominated by the resonant current. In M3, the rectifier switches off and  $C_{out}$  is being charged, and so  $i_{C_{out}}$  and its scaled version  $v_A$  increase accordingly.  $v_A$  and  $v_B$  are combined to reconstruct the estimated current  $v_e$ , and are used to generate the feedback signal  $v_{zC}$  for the PLL controller.

### 3.2. ZVS PLL controller

The PLL controller is implemented by a CMOS CD4046 to lock-on to the resonant current and generate in-phase gate signals to achieve ZVS. The CD4046 circuit contains a voltage-controlled oscillator (VCO) and a phase comparator and requires an external low-pass filter (LPF), as shown in Fig. 6. The operating frequency range of the VCO is controlled by an external timing capacitor and two timing resistors. The type II phase comparator of CD4046 is used to synchronise both phase and frequency of the input signals and generate an error signal for the LPF. In most PLL circuits, when locked the phase and frequency of VCO output should be matched to the input signal. In this application, however, a frequency divider is employed within the phase detector loop so that the VCO is actually locked to twice the resonant current frequency. With appropriate logic the  $f_{lock}$  (A) and  $f_{lock/2}$  (B) signals allow a complete cycle to be divided into four equal sections of

duration  $90^\circ$  or  $\pi/2$  radians. The Boolean equations (3) and (4) show how the signals A and B may be decoded to provide the necessary gate drive to meet the critical criterion. Switching waveforms shown in Fig. 7 demonstrate successful operation of the PLL controller for achieving ZVS as resonant current is locked on and gate drive signals are phase- and frequency-matched to  $i_{L1}$ .

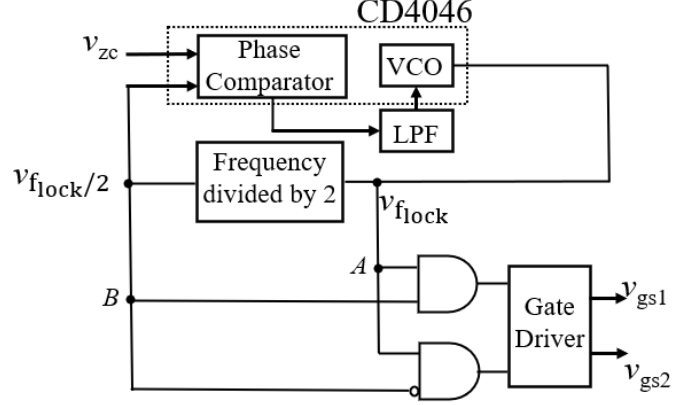


Fig. 6: Block diagram of the proposed ZVS PLL controller

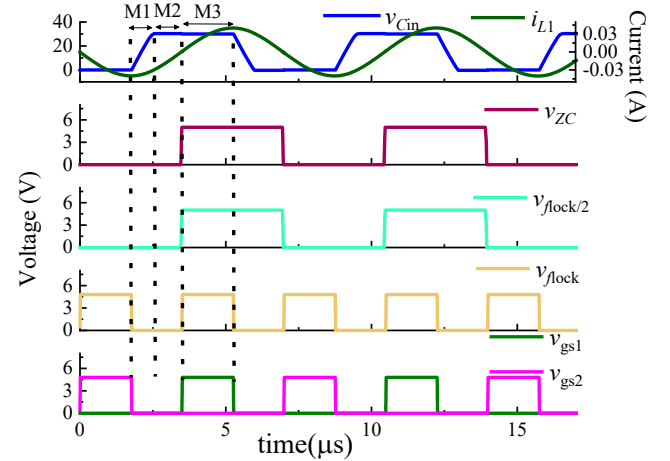


Fig. 7: Operating waveforms of ZVS PLL controller

$$v_{gs1} = A \cdot B \quad (3)$$

$$v_{gs2} = A \cdot \bar{B} \quad (4)$$

### 3.3. Burst-mode control

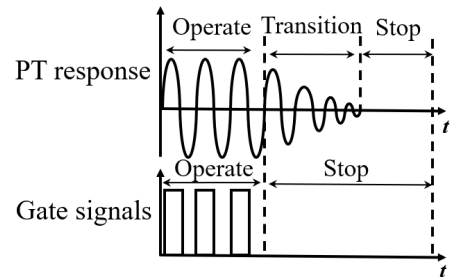


Fig. 8: Gate signals and PT response with burst mode modulation

To regulate the output voltage, the power supply operates in burst mode by controlling the on/off periods of MOSFETs according to regulation requirement. A typical PT response in burst-mode modulation is shown in Fig. 8. As can be seen, the

PT doesn't stop instantly when the switches are turned-off due to its mechanical vibration. Therefore, a transition period occurs and introduces a time delay in the control.

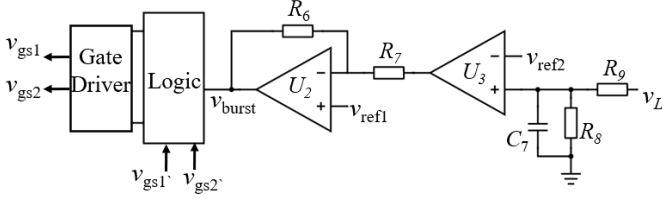


Fig. 9: Circuit diagram of burst-mode hysteresis operation

The burst-mode operation is accomplished by the hysteresis window through a burst signal  $v_{burst}$  to obtain a good converter dynamic response. The burst signal  $v_{burst}$  is generated from a hysteresis window with upper and lower voltage regulation limits. Thus, PT drive stops when  $v_L$  meet the upper limit and it starts to operate again at the lower boundary. As shown in Fig. 9, a Schmitt trigger comparator  $U_2$  is used to implement the hysteresis window, and the window size is determined by  $R_6$ ,  $R_7$  and reference signal  $v_{refl}$ . The output voltage  $v_L$  is adjusted and filtered before applied to the hysteresis comparator.

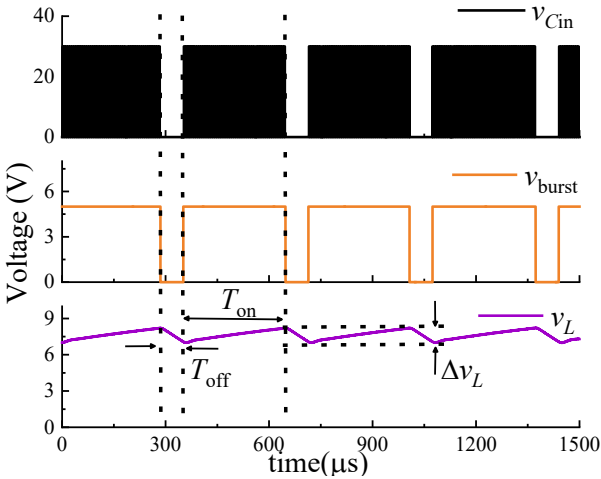


Fig. 10: Operating waveforms of the burst-mode control

Fig. 10 Shows the switching waveforms of the resonant converter under burst-mode operation. During burst mode operation, the piezoelectric transformer is considered to be a current source  $I_{piezo}$  that charges the filter capacitor  $C_f$  until  $v_L$  reaches the upper regulation limit and the load discharges  $C_f$  until  $v_L$  reaches the lower boundary. As can be seen from Fig. 10,  $\Delta v_L$  is the voltage ripple and is controlled by the on/off periods of the switches through hysteresis window. The on and off time of burst-mode operation are indicated as

$$T_{on} = \frac{C_f \Delta v_L}{I_{piezo} - I_L} \quad (5)$$

$$T_{off} = \frac{C_f \Delta v_L}{I_L} \quad (6)$$

where  $I_L$  is the load current. When PT operates continuously without burst mode modulation,  $I_{piezo}$  equals to  $I_L$ . Therefore, the burst frequency  $f_{burst}$  can be found from equation (5) and (6)

$$f_{burst} = \frac{(I_{piezo} - I_L)I_L}{C_f \Delta v_L I_{piezo}} \quad (7)$$

As can be seen from equation (7), for a given PT and filter capacitor, the voltage ripple  $\Delta v_L$  is inversely proportional to  $f_{burst}$ . Therefore, the burst frequency should be increased if a smaller  $\Delta v_L$  is required or a large value for  $C_f$  must be used.

## 4. Experimental results

To validate the proposed control method, a prototype half-bridge PT-based resonant converter is implemented and tested as shown in Fig. 11(a). A ring-dot radial-mode PT with a natural frequency of 140 kHz is used for the test, as shown in Fig. 11(b), with the extracted equivalent circuit component values given in table I.

The experimental waveforms of the proposed control circuit are shown in Fig. 12. To ensure adequate lock range with acceptable component tolerance, the PLL is restricted to operate between 270kHz to 290kHz (i.e. in the range of twice the resonant frequency of the PT). A 810  $\Omega$  load (corresponds to 1 k $\Omega$  matched load at PT output) is used to validate the proposed controller, since this is the worst operating condition for achieving ZVS.

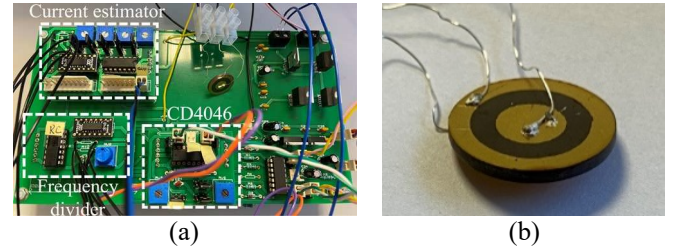


Fig. 11: Experimental set-up of the proposed control system. (a) prototype PT-based inductorless converter with proposed control circuit and (b) PT under test.

Table 1: PT equivalent circuit parameters

$C_{in}$	$C_{out}$	$L_1$	$C_1$	$R_1$	$N$	$Q$
0.43nF	1.14nF	17.2mH	77.8pF	12.5 $\Omega$	0.94	1190

As can be seen from Fig. 12(a), the phase comparator input signals  $v_{zc}$  and  $v_{flock}$  are frequency- and phase-matched, demonstrating a PLL locked-on condition. The resonant current is estimated by  $v_A$  and  $v_B$ , reconstructed as  $v_e$  and modified to  $v_{zc}$ , clearly indicating the zero crossings for ZVS operation. The gate drive signals are generated through steering logic with  $\pi/2$  deadtime and align with the feedback signal  $v_{zc}$ . ZVS is clearly achievable since  $v_{Cin}$  reaches  $V_{dc}$  during the deadtime period.

Fig. 12(b) shows the circuit output voltage regulation performance. A 3kHz burst signal  $v_{burst}$  is set by the hysteresis window to achieve 7.5V output with 300mV voltage ripple. According to the experimental measurement, the transition time for PT starts and stops are 5 and 12 PT resonant periods, respectively. The transition times are measured between the burst signal switching instant and  $v_{Cin}$  reaches steady state.

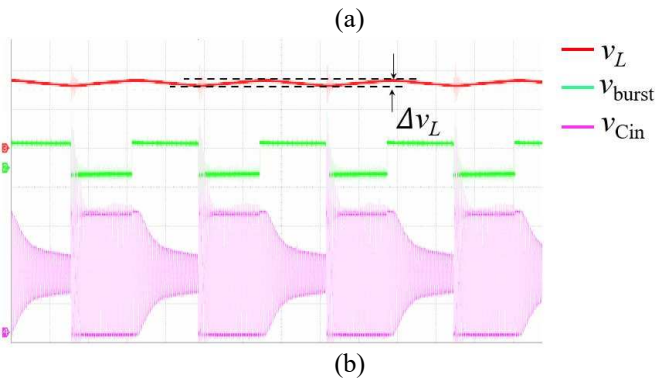
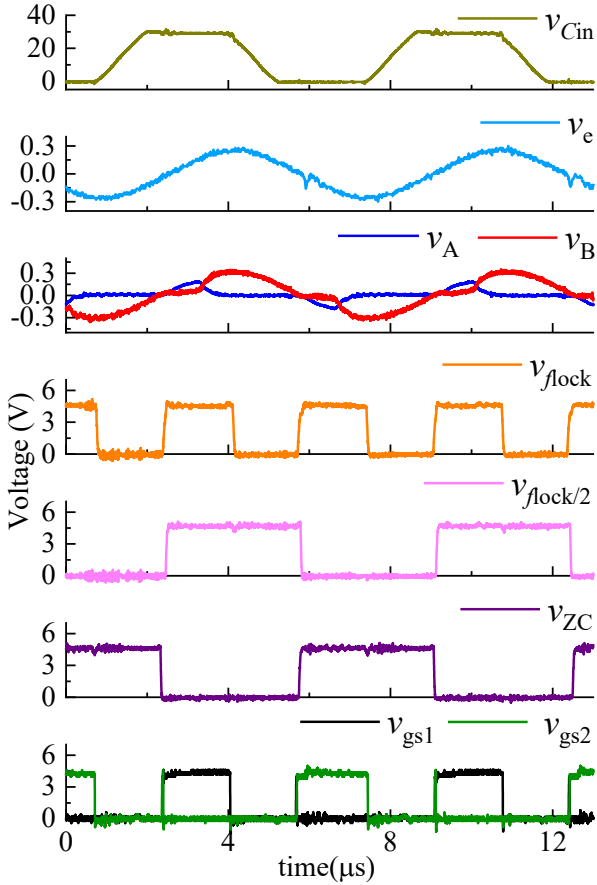


Fig. 12: Experimental measurements of the prototype converter and control circuit. (a) PLL controller associated with frequency divider under ZVS operation and (b) output voltage regulation by burst-mode hysteresis control at the matched load condition. (PT input capacitance voltage  $v_{Cin}$  10V/div, burst signal  $v_{burst}$  5V/div and output voltage  $v_L$  5V/div).

## 5. Conclusion

Output voltage regulation and ZVS operation of a PT-based inductorless half-bridge converter is presented in this paper. A ring dot radial mode PT is used to verify the proposed control circuit at matched load condition. A secondary-side resonant current estimator has been demonstrated to accurately reconstruct an unmeasurable signal and ZVS is achieved by using a PLL to lock onto this signal. Voltage regulation has been accomplished by burst mode control through a hysteresis window. The output voltage is restricted by the window size

and the gate signals are modulated by the corresponding burst signal via PLL controller and logic circuit. Therefore, the MOSFETs are periodically switched on/off to satisfy regulation requirements.

## 6. References

- [1] Wang, Y. C., He, J. J., Liu, Y. P., Wu, Y. P., Lee, C. K., Huang, Y. T., "Theory and experiment of high voltage step-up ratio disk type piezoelectric transformer for LCD-TV", Proc. IEEE Int. Conf. Mech, Taiwan, 2005, pp. 284-287.
- [2] Rødgaard, M. S., Weirich, M., Andersen, M. A. E., "Forward conduction mode controlled piezoelectric transformer-based PFC LED drive," IEEE Trans. Power Electron., 2013, 28, (10), pp. 4841-4849.
- [3] Hutsel, B. T., Kovaleski, S. D., Kwon, J. W., "Optimization of piezoelectric resonance effect in a piezoelectric transformer plasma source", IEEE Trans. Plasma Sci., 2013, 41, (2), pp. 305-311.
- [4] Foster, M. P., Davidson, J. N., Horsley, E. L., Stone, D. A., "Critical Design Criterion for Achieving Zero Voltage Switching in Inductorless Half-Bridge-Driven Piezoelectric-Transformer-Based Power Supplies", IEEE Trans. Power Electron., 2016, 31, (7), pp. 5057-5066.
- [5] Z. Yang, J. N. Davidson and M. P. Foster, "Output voltage regulation for piezoelectric transformer-based resonant power supplies using phase-locked loop," 10th Inter. Conf. Power Electronics, Machines and Drives (PEMD 2020), pp. 455-460, 2020.
- [6] Z. Yang, J. Forrester, J. N. Davidson, M. P. Foster and D. A. Stone, "Resonant current estimation and phase-locked loop feedback design for piezoelectric transformer-based power supplies", IEEE Transactions on Power Electronics, vol. 35, no. 10, pp. 4666-4676, 2020.
- [7] Chen, S.Y., Chen, C.L., "ZVS Considerations for a Phase-Lock Control DC/DC Converter with Piezoelectric Transformer", 32nd Ann. Conf. IEEE Ind. Electron., Paris, France, April 2007.
- [8] Liu, Y. P., Vasic, D., Costa, F., Wu, W. J., Lee, C. K., "Design of fixed frequency controlled radial-mode stacked disk-type piezoelectric transformers for DC/DC converter applications", Smart Materials and Structures, 2009, 18, (8).
- [9] Horsley, E. L., "Modelling and Analysis of Radial Mode Piezoelectric Transformers and Inductor-less Resonant Power Converters", Ph.D Thesis, Department of Electrical and Electrical Engineering, University of Sheffield, 2011.